Journal of Computers Vol. 31 No. 3, 2020, pp. 1-10
doi:10.3966/199115992020063103001

Fault Diagnosis of Rotating Machinery Based on Dimensionless Index and Two-sample Distribution Test

Nai-quan Su[1,2], Xiao Li[2], Qing-hua Zhang[1*], Chong-lin Huang[3]

[1] Guangdong Provincial Key Lab.of Petrochemical Equipment and Fault Diagnosis,
Guangdong University of Petrochemical Technology, Maoming 525000, China
534306286@qq.com, fengliangren@163.net

[2] School of Electromechanical Engineering, Guangdong University of Technology,
Guangzhou 510006, China
534306286@qq.com

[3] School of Electromechanical Engineering, Guangdong University of Petrochemical Technology,
Maoming, 525000, China
651867429@qq.com

Received 28 August 2018; Revised 10 February 2019; Accepted 6 March 2019

Abstract. Dimensionless indexes are used to identify the faults type of rotating machinery, there is an overlap between the dimensionless index ranges of each fault, and result in poor fault diagnosis. So in this paper, an algorithm is proposed a dimensionless indexes and two-sample distribution test. This method are compared the cumulative probability distribution function between the known fault samples and the tested fault samples, and find out the maximum statistical distance. According to the similar degree of the two samples, and the tested fault sample is able to be diagnosed. The method is applied in the simulation experiment of petrochemical unit show that the method is simple and effective, and it has the strong fault identification ability to extract the fault feature accurately. This provides the guidance for rotating machinery fault diagnosis and other large equipment.

Keywords: dimensionless indexes, experimental verification, fault diagnosis, two-sample distribution test

1 Introduction

Rotating machinery such as gears, bearings and shafts in large units usually work in complex environments. Its vibration signals tend to be nonlinear, random and non-ergodic, making it difficult to identify fault signals. When faults occur with large units, a complete shutdown and inspection is required, and resulting in huge economic losses [1-3]. Therefore, accurately identifying of single and composite faults is of great economic and technical significance.

The dimensionless method is insensitive to disturbances in the vibration signal of rotating machinery, and the amplitude and frequency of the signal are relatively stable. It has been widely used in fault diagnosis of rotating machinery [4-6]. This method is to identify fault types by calculating five dimensionless indexes of normal state and fault state. When the fault occurs, the maximum and minimum values of each DI are used as the critical value of the equipment [7-9]. However, there is a certain overlap between the range of the normal state or various fault states, resulting in fault types are difficult to be distinguished. [10-11] proposed a genetic programming method based on the DI, which achieved good results in the classification of fault types. [12-14] proposed a SVM method is applied to some complicated optimization problems. However, it needs to spend a long time to complete the training task

* Corresponding Author

[15]. [16-17] proposed a small sample method applying for LDA processing. [18] proposed two-dimensional distributed entropy for small sample data feature representation, and uses its characteristics that are not sensitive to rotation. [19-20] proposed small sample method is applied to classification of fault types. However, small sample method has over fitting problem. In order to solve this problem, [21] proposed domain adaptive fault diagnosis based on the geodesic flow kernel under small data condition, to overcome shortage of prior faulty data or the incompleteness of sample space. [22] proposed a fluctuation detection and fault diagnosis method, to tackle the shortage of existing instantaneous frequency evaluation. [23] proposed DBN and Teager-Kaiser energy operators a fault diagnosis method for reciprocating compression valves. [24] proposed Fuzzy If-Then rules deal with fuzzy uncertainties. However, these methods do not handle uncertain probabilities very well. [25] proposed a VANET and machine learning, to recognize the abnormal traffic state. [26] builds a new fault analysis model on RSA using square and multiply, improved fault analysis.

The author believes that solving the overlap between the ranges of each DI. It is possible to judge whether they are from the same population by judging the similarity of two independent statistical samples. Based on this, a method that is two-sample distribution test (TSDT) is proposed. Firstly, the dimensionless method is used to obtain the five DI ranges. Then, we are compared the cumulative probability distribution functions of the known fault samples with the tested fault samples, and obtain statistical distance. Finally, the fault types are determined according to obtained maximum statistical distance. The method can effectively solve the overlap problem between the DI ranges, and improve the ability to identify faults. The simulation experiment shows that the method is effective.

The main contributions in this paper are concluded as follows:

- We propose a method for fault diagnosis of rotating machinery based on dimensionless indexes and two-sample distribution test.
- The method proposed in this paper can effectively solve the overlap problem between the DI ranges.
- It is verified with a large petrochemical unit simulation experiment system, and is shown to be effective.

This paper is divided into five chapters: The first chapter is a brief introduction, the basic introduction to the research motive and the main contributions in this paper; The second chapter mainly describes the process of fault diagnosis; The third chapter introduces the dimensionless algorithm and the TSDT; The fourth chapter is experimental verification of the proposed method; The fifth chapter is conclusion and future prospect.

2 The Proposed Method

The TSDT is based on the dimensionless method. Firstly, the fault vibration time domain signal is collected and classified, and then the dimensionless method is used to calculate, to obtain DI ranges. Secondly, the cumulative probability distribution function are compared the known fault sample with the tested fault sample, and the maximum statistical distance is obtained. Finally, fault types identification according to the minimum principle of the maximum statistical distance. The TSDT method for fault diagnosis is shown in Fig. 1.

3 The Theoretical Basis

3.1 Dimensionless Indexes (DI)

Dimensionless is the ratio of two quantities of the same dimension. The basic idea is to achieve dimensionless by comparing the ratios of two dimensions used the probability density function. Therefore, the dimensionless is immune to the mechanical signal frequency and amplitude in fault diagnosis [27-28]. The dimensionless algorithm is defined as follows:

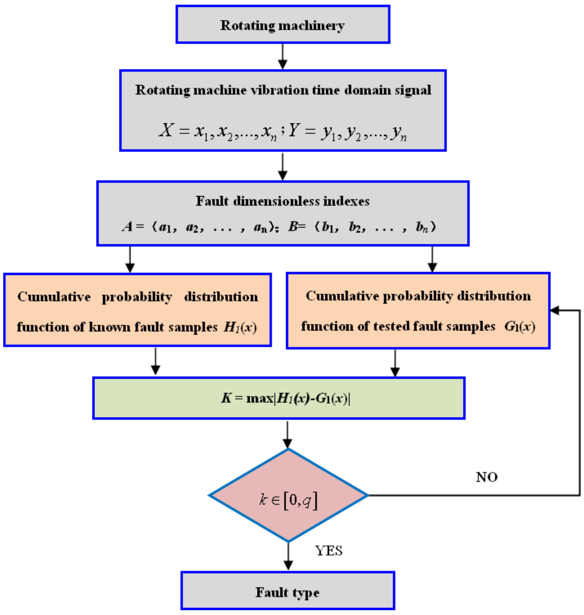

Fig. 1. The fault diagnosis process of two- sample distribution test

$$\zeta_x = \frac{\left[\int_{-\infty}^{+\infty} |x|^l \, p(x)dx\right]^{\frac{1}{l}}}{\left[\int_{-\infty}^{+\infty} |x|^m \, p(x)dx\right]^{\frac{1}{m}}} \tag{1}$$

In the formula: x is the amplitude of the vibration random time domain signal. $p(x)$ is the probability density function of the amplitude x. l and m are the numerator and denominator coefficients. DI: waveform index, peak index, pulse index, margin index and kurtosis index as shown in Table 1 [4].

Table 1. Dimensionless parameter

DI	Molecular l and denominator m coefficient	calculation formula
Waveform index	$l = 2, m = 1$	$S_f = \frac{\left[\int_{-\infty}^{+\infty} \lvert x\rvert^2 \, p(x)dx\right]^{\frac{1}{2}}}{\left[\int_{-\infty}^{+\infty} \lvert x\rvert \, p(x)dx\right]} = \frac{X_{rms}}{\lvert X\rvert}$
Pulse index	$l \to \infty, m = 1$	$I_f = \frac{\left[\int_{-\infty}^{+\infty} \lvert x\rvert^l \, p(x)dx\right]^{\frac{1}{l}}}{\left[\int_{-\infty}^{+\infty} \lvert x\rvert \, p(x)dx\right]} = \frac{X_{\max}}{\lvert X\rvert}$
Margin index	$l \to \infty, m = \frac{1}{2}$	$CL_f = \frac{\left[\int_{-\infty}^{+\infty} \lvert x\rvert^l \, p(x)dx\right]^{\frac{1}{l}}}{\left[\int_{-\infty}^{+\infty} \lvert x\rvert^{\frac{1}{2}} \, p(x)dx\right]^2} = \frac{X_{\max}}{X_r}$
Peak index	$l \to \infty, m = 2$	$C_f = \frac{\left[\int_{-\infty}^{+\infty} \lvert x\rvert^l \, p(x)dx\right]^{\frac{1}{l}}}{\left[\int_{-\infty}^{+\infty} \lvert x\rvert^2 \, p(x)dx\right]^{\frac{1}{2}}} = \frac{X_{\max}}{X_{rms}}$
Kurtosis index	N/A	$K_v = \frac{\int_{-\infty}^{\infty} x^4 p(x)dx}{\left(\int_{-\infty}^{\infty} x^2 p(x)dx\right)^2}$

In the formula: x is the amplitude. $p(x)$ is the probability density function of the amplitude. β is the kurtosis. X_{max} is the maximum. X_r is the square root amplitude. X_{rms} is the root mean square value. $|X|$ is average amplitude.

The vibration time domain signal amplitude of the known fault samples $X = (x_1, x_2, ..., x_n)$ and the tested fault samples $Y= (y_1, y_2, ..., y_n)$. The DI of the known fault samples is defined as follows:

$$\zeta_x = \frac{\left[\int_{-\infty}^{+\infty} |X|^l p(X)dx\right]^{\frac{1}{l}}}{\left[\int_{-\infty}^{+\infty} |X|^m p(X)dx\right]^{\frac{1}{m}}} = a_n \tag{2}$$

The DI of the tested fault samples is defined as follows:

$$\zeta_y = \frac{\left[\int_{-\infty}^{+\infty} |Y|^l p(Y)dx\right]^{\frac{1}{l}}}{\left[\int_{-\infty}^{+\infty} |Y|^m p(Y)dx\right]^{\frac{1}{m}}} = b_n \tag{3}$$

In the formula, n is the number of DI.

The DI of the known fault samples calculated by formula (2) and (3) $A = (a_1, a_2, ..., a_n) \in [c, d\,]$, and the DI of the tested fault sample $B = (b_1, b_2, ..., b_n) \in [e, f\,]$. c and d respectively are the minimum and maximum values of the known fault samples, e and f respectively are the minimum and maximum values of the tested fault samples.

3.2 Two-sample Distribution Test (TSDT)

The cumulative frequency of the known fault samples $M = (F_{a1}(x), F_{a2}(x),..., F_{an}(x))$, and the tested fault samples $N = (R_{b1}(x), R_{b2}(x),..., R_{bn}(x))$. The statistical distance for each cumulative frequency is defined as follows:

$$\begin{aligned} Dist(M,N) &= F_{a_1}(x) - F_{b_1}(x) = \frac{F_1}{n} - \frac{R_1}{n} = D_1 \\ Dist(M,N) &= F_{a_2}(x) - F_{b_2}(x) = \frac{F_2}{n} - \frac{R_2}{n} = D_2 \\ &\vdots \\ Dist(M,N) &= F_{a_n}(x) - F_{b_n}(x) = \frac{F_n}{n} - \frac{R_n}{n} = D_n \end{aligned} \tag{4}$$

After comparing M with N, the statistical distance is $W_{\mathrm{n}}= (D_1, D_2, ..., D_{\mathrm{n}})$, and the specific value range is as follows:

$$W_n = \begin{cases} \gamma, \; other \\ 1, \; if \quad F_{a_n} = 1 \;\; and \;\; F_{b_n} = 0 \;\; or \;\; F_{a_n} = 0 \;\; and \;\; F_{b_n} = 1 \\ 0, \; if \quad F_{a_n} \;\; and \;\; F_{b_n} \;\; same \end{cases} \tag{5}$$

Assuming that the cumulative probability distribution function of the known fault sample is $H_1(x)$, and the tested fault sample is $G_2(x)$. Comparing the known fault sample with the tested fault sample, and obtaining the maximum statistical distance k is defined as follows:

$$\begin{aligned} k &= \max\left|H_1(x) - G_2(x)\right| \\ &= \max\left|\frac{F_n}{n} - \frac{R_n}{n}\right| \end{aligned} \tag{6}$$

After compare $H_1(x)$ with $G_2(x)$, the specific values of k is defined as follows:

$$k = \begin{cases} \gamma \in (0,1], & other \\ 0, & if \quad H_1(x) \quad and \quad G_2(x) \quad same \end{cases} \tag{7}$$

Conclusion: The k value is represent the maximum statistical distance between the known fault samples and the tested fault samples. If $k \in [0,q]$, it means that the two samples belong to the same distribution. Flow chart of algorithm diagnosis is shown in Fig. 2.

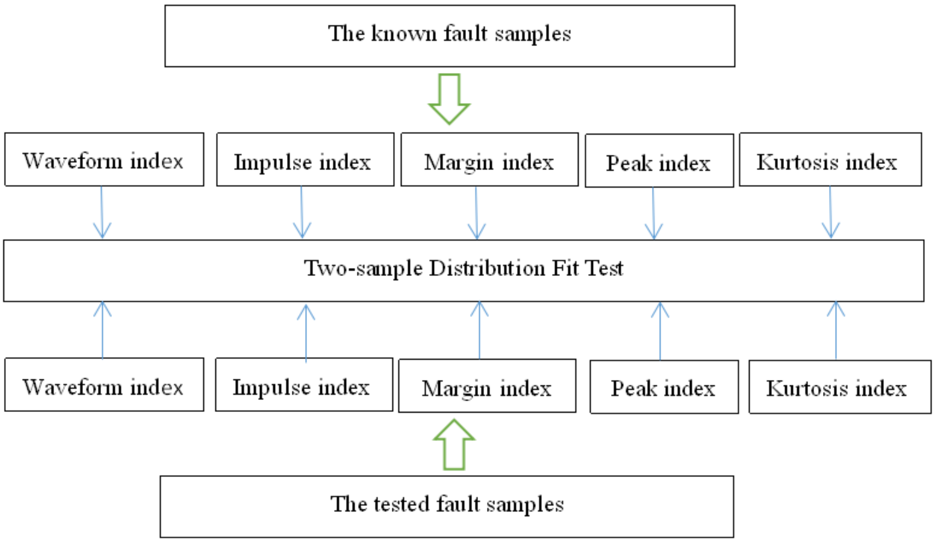

Fig. 2. Flow chart of algorithm diagnosis

3.3 Fault Identification Process

The process of DI and TSDT, the proposed method is described below:

Step 1: Collecting the vibration time-domain signal of the rotating machinery. The amplitude of the known fault sample vibration time-domain signal is $X = (x_1, x_2, ..., x_n)$, and the amplitude of the tested fault sample is $Y = (y_1, y_2, ..., y_n)$.

Step 2: The dimensionless algorithm is able to process the vibration time-domain signal, and obtain five DI, according to Eqs. (1) - (3) and Table 1. The dimensionless indexes of the known fault samples: $A = (a_1, a_2, ..., a_{n)}$, and the tested fault samples are $B = (b_1, b_2, ..., b_n)$.

Step 3: According to A and B in step 2, the cumulative frequency of the known fault samples $M = (F_{a1}(x), F_{a2}(x), ..., F_{an}(x))$, and that the cumulative frequency of the tested fault samples $N = (R_{b1}(x), R_{b2}(x), ..., R_{bn}(x))$.

Step 4: The maximum statistical distance of the known fault samples and the tested fault samples: $k = (k_1, k_2, ..., k_n)$ according to Eqs. (4) - (7).

4 Experimental Verification

4.1 Experimental Signal Acquisition and Processing

In order to verify the effectiveness of TSDT in fault diagnosis, it is applied to the petrochemical large unit simulation experiment system.

The simulation experiment system consists of a multi-stage centrifugal air compressor unit, test benches and test software. The test software can display the time domain of the unit's vibration time domain signal in real time. It can store historical data while monitoring the signal characteristics and monitor the operation of the unit. Fig. 3 shows the test bench of multi-stage centrifugal air compressor unit fault diagnosis. Fig. 4 shows the experimental defect parts. Table 2 shows the model and parameters of the main components.

Fig. 3. Laboratory furniture of multistage centrifugal air compressor

(a) Gear teeth shortage (b) Bearing inner ring wear (c) Bearing lack of ball (d) Bearing outer ring wear

Fig. 4. Experimental fault

Table 2. The main parts of the experimental unit

Equipment	model	parameter
Inverter motor	YP-50-112	Triangular junction Circuit; Rated voltage, current and power are 380 *V*, 24.8 *A* and 11 *Kw*, respectively.
Multistage centrifugal fan	C8-2000	Rated power 11*Kw*; Maximum speed 2970 *r*/*min*; blowing rate 8 m^3/min.
Torque sensor	CYT-302	Rated torque 100 *N.m*; Speed range 0~3000 *r*/*min*; Temperature coefficient: -0.027%/℃; Precision: ±0.2%*FS*.
Data collector	EMT390	Acceleration 0.1~199.9 m/s^2; Acquisition frequency 10 *Hz*~10 *KHz*; Number of groups 1~100; Sampling points 512、1024、2048 etc.

In the experiments, the EMT390 data collector is used to collect the vibration time-domain signal. In the experiment, the unit is calibrated. Firstly, The vibration time domain signal is collected in normal state. Then the fault defect part is replaced, and followed by the collection of 100 sets of vibration time domain signal under each fault condition. The test conditions are as follows: motor speed is 1000 *r*/*min*.

The following is how to verify the effectiveness of the algorithm in petrochemical rotating machinery. Firstly, the DI is calculation by algorithm, and the waveform index, peak index, pulse index, margin index and kurtosis index range of the tested fault samples are obtained. Then, the maximum statistical distance k value is obtained by TSDT. Finally, the tested fault samples are judged according to k value. If the similarity between the known fault sample and the tested fault sample are reached to 95%, indicates that the two samples belong to the same distribution. The test result is showed “YES”. Otherwise, the cumulative probability distribution function of the two samples is different, and the test result is showed “NO”, indicating that the fault types occurred is different.

Fig. 5 shows the vibration time domain signal amplitude of single and composite faults. According to formula (6) to process the vibration time domain signal of the rotating machinery by the dimensionless algorithm, the range of five DI is shown in Table 3.

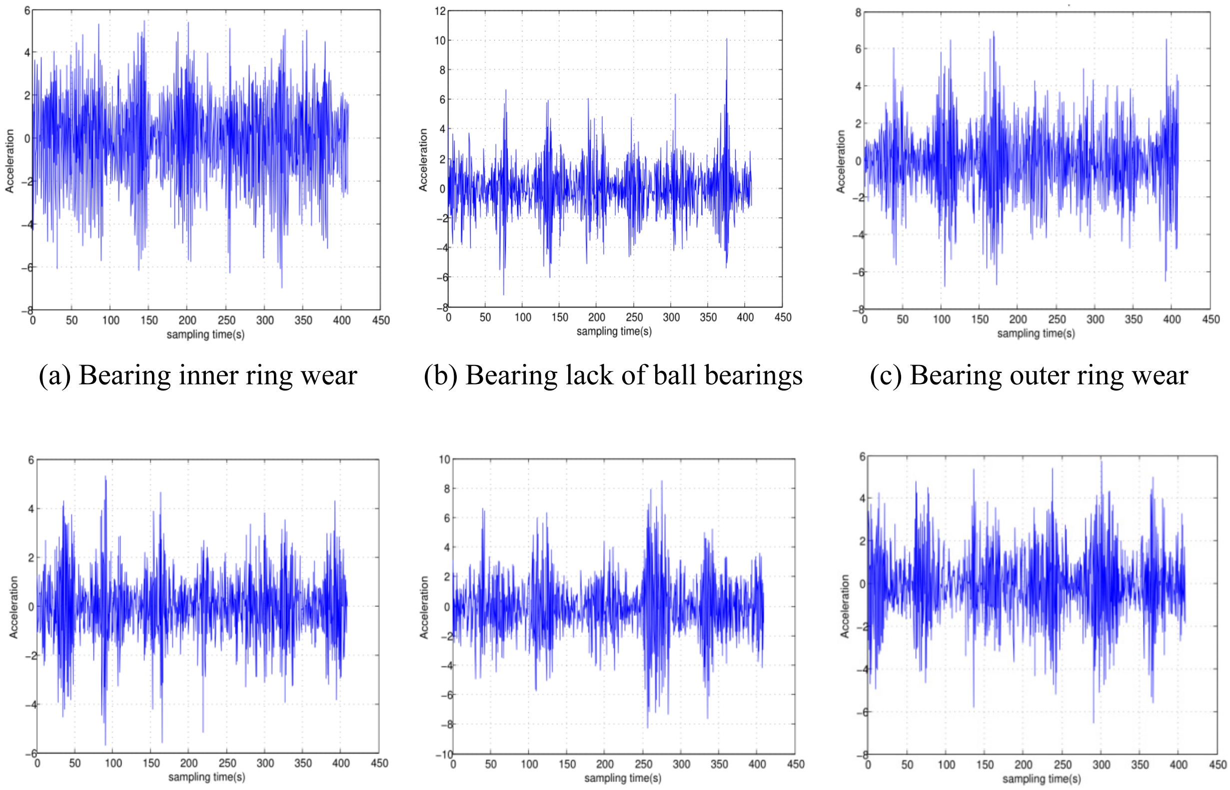

(a) Bearing inner ring wear (b) Bearing lack of ball bearings (c) Bearing outer ring wear

(d) Gear teeth shortage and bearing outer ring wear (e) Gear teeth shortage and bearing inner ring wear (f) Gear teeth shortage and bearing lack of ball

Fig. 5. Different faults, vibration time domain signal amplitude

Table 3. The range of five DI

Known fault type	Wave form index	Impulse index	Margin index	Peak index	Kurtosis index
Bearing lack of ball	[1.2749 1.4014]	[4.1639 8.8194]	[5.0155 11.032]	[3.1991 6.2933]	[5.0155 11.032]
Bearing outer ring wear	[1.2378 1.3244]	[2.1364 5.7622]	[2.4956 6.9185]	[1.7260 4.4521]	[2.9204 4.2267]
Bearing inner ring wear	[1.2367 1.3136]	[3.0448 4.4409]	[3.5740 5.3579]	[2.4408 3.4556]	[2.7225 3.8396]
Gear teeth shortage and bearing outer ring wear	[1.2483 1.3307]	[3.8598 8.5111]	[4.5854 10.142]	[2.9523 6.5810]	[3.0641 5.2534]
Gear teeth shortage and bearing inner ring wear	[1.2792 1.3856]	[3.9166 6.9788]	[4.7670 8.6456]	[2.9950 5.1692]	[3.3202 5.6898]
Gear teeth shortage and bearing lack of ball	[1.2725 1.4070]	[3.6735 7.3948]	[4.3973 9.1293]	[2.8652 5.4168]	[3.2681 5.4565]

4.2 Analysis of Experimental Results

The tested fault samples and the known fault samples are calculated according to formula (6), and obtain a line chart with the maximum statistical distance k as shown in Fig. 6.

Sf: Waveform index. If: Impulse index. CLf: Margin index. Cf: Peak index. Kv: Kurtosis index.

Fig. 6 is aiming at a problem of the poor diagnostic results for which the overlap between the range of DI for single faults. The maximum statistical distance obtained according to the TSDT. It can identify the single fault according to the minimum value k of the five DI. It can be seen from Fig. 6 that the same single faults are compared with each other to obtain the smallest k value. From the distribution of the line chart, the faults occurring in the tested fault sample can be identified easily and accurately. Fig. 6 is described below:

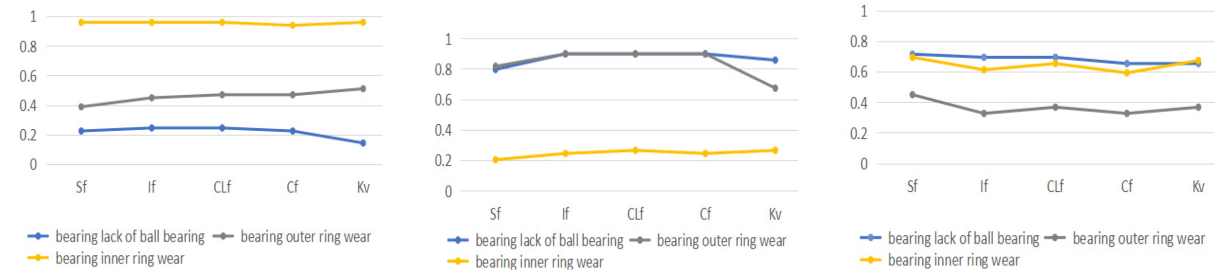

(a) Bearing lack of ball bearings (b) Bearing inner ring wear (c) Bearing outer ring wear

Fig. 6. Single fault samples, line chart of maximum statistical distance

Bearing lack of ball bearings: The three fold line graphs are clearly separated, bearing lack of ball bearings compared with the tested fault sample to obtain the maximum statistical distance. The sample fault is bearing lack of ball bearing.

Bearing inner ring wear: The two fold lines overlap each other, we can identify the fault diagnosis based on the maximum statistical distance, and these five values of *k* are smaller than other faults. The sample fault is gears teeth missing and bearing outer ring.

Bearing outer ring wear: There are two points overlap in the two fold lines, the five *k* values of bearing outer ring wear are smaller than the other two known fault samples. The sample fault is bearing outer ring wear.

Table 3 shows that composite fault is a large overlap between DI ranges. In order to further verify the diagnostic effect of the composite faults. The composite fault samples are selected, and the maximum statistical distance for each fault by TSDT, it can be seen from Fig. 7. Although there is a small overlap of the line chart of the composite faults, the method can completely identify the types of the composite faults by the distribution of the line chart and the minimum *k* value. Fig. 7 is described below:

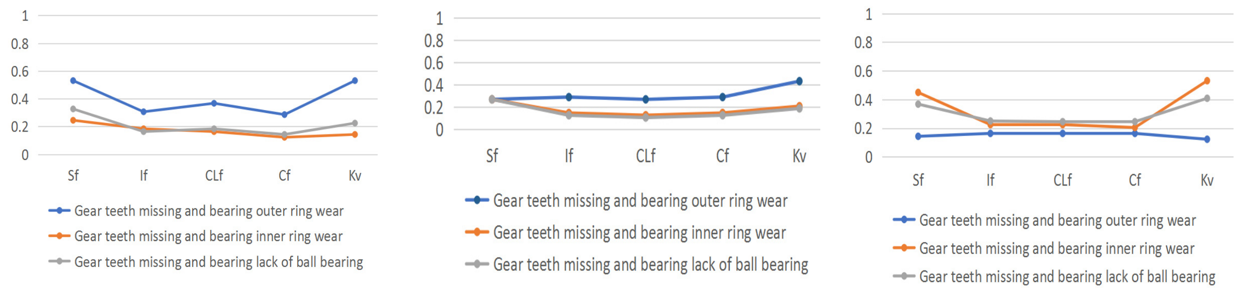

(a) Gear teeth missing and bearing inner ring wear (b) Gear teeth missing and bearing lack of ball (c) Gear teeth missing and bearing outer ring wear

Fig. 7. Composite fault samples, line chart of maximum statistical distance

Gear teeth missing and bearing inner ring wear: The two fold lines overlap each other. Therefore, the fault type is identified based on the distribution of the three fold lines. The sample fault is gear teeth missing and bearing inner ring wear.

Gear teeth missing and bearing lack of ball: There are two fold lines close to coincide, which makes it difficult to diagnose fault types. We identify the fault types according to these five minimum values. The sample fault is gear teeth missing and bearing lack of ball.

Gear teeth missing and bearing outer ring wear: There is a folding line at the bottom, according to the distribution of the three fold lines, to identify the fault types. The sample fault is gear teeth missing and bearing outer ring wear.

5 Conclusions

In this paper, two-sample distribution test (TSDT) is proposed. It is effectively solve the overlap problem of the DI range of the fault state. Experiments in the petrochemical large unit simulation experiment system show the maximum statistical distance between the cumulative probability distribution function of the known fault sample and the tested fault sample, its ability to effectively identify fault types. In the tested fault samples, the accuracy rate reached 100%, which explain the method plays a guiding role in the fault diagnosis of rotating machinery for petrochemical large units and other large equipment. In the future work, we would further study the superiority of this method compared with other methods, and applicability in the real applications.

Acknowledgments

The research was partially supported by the Key Project of Natural Science Foundation of China (Grant No. 61933013) and the National Nature Science Foundation of China (Grant Nos. 61673127, 61973094). The work described in this paper was also partially supported by the Key Project of Natural Science Foundation of Guangdong (Grant No. 2018B030311054) and Guangdong University key platform Youth Innovative Talents Project (2019KQNCX085).

References

[1] D.H. Zhou, Y. Liu, X. He, Review on fault diagnosis techniques for closed-loop systems, Acta Automatica Sinica 39(11)(2013) 1933-1943.

[2] Z.W. Gao, C. Cecati, S.X. Ding, A survey of fault diagnosis and fault tolerant techniques- Part I: fault diagnosis with model-based and signal-based approaches, IEEE Transactions on Industrial Electronics 62(6)(2015) 3757-3767.

[3] L.L. Jiang, H.K. Yin, X. Li, Fault diagnosis of rotating machinery based on multisensor information fusion using SVM and time-domain features, Shock Vibrat 1(2014) 153-154.

[4] J.B. Xiong, Q. Liang, J.F. Wan, Q.H. Zhang, X.H. Chen, R.B. Ma, The order statistics correlation coefficient and PPMCC fuse non-dimension in fault diagnosis of rotating petrochemical unit, IEEE Sensors Journal 18(11)(2018) 4704-4714.

[5] J. Yuan, Y. Wang, Y. Peng, Weak fault detection and health degradation monitoring using customized standard multiwavelets, Mechanical Systems and Signal Processing 94(2017) 384-399.

[6] A.L.R. Sibrant, E. Mittelstaedt, A. Davaille, Accretion mode of oceanic ridges governed by axial mechanical strength, Nature Geoscience 11(2018) 274-279.

[7] D.L. Cui, Q.H. Zhang, M. Xiao, Feature spectrum extraction algorithm for rolling bearings based on spectrogram and constrained NMF, Bearing 5(2014) 48-52.

[8] J.J. Chen, B. Xu, Fault diagnosis for rolling bearing based on the non-dimensional parameter and spectrum analysis, Mach Design Res 31(4)(2015) 75-77.

[9] X. Dai, Z. Gao, From model signal to knowledge: a data-driven perspective of fault detection and diagnosis, IEEE Trans 9(4)(2013) 2226-2238.

[10] Q. Hu, Q.H. Zhang, A.S. Qin, The application of genetic programming design in fault classification of rotating machinery, Computer Applications and Software 30(10)(2013) 57-59.

[11] H. Guo, L.B. Jack, A.K. Nandi, Feature generation using genetic programming with application to fault classification, IEEE Transactions on Systems Man & Cybernetics Part B Cybernetics A Publication of the IEEE Systems Man & Cybernetics Society 35(1)(2005) 89-99.

[12] L. ozgur, T. Gungor, Two-stage feature selection for text classification, in: O.H. Abdelrahman, E. Gelenbe, G. Gorbil, R. Lent (Eds.), Information Sciences and Systems 2015: 30th International Symposium on Computer and Information Sciences (ISCIS 2015), Springer, 2015, pp. 329-337. doi:10.1007/978-3-319-22635-4_30.

[13] S. Kim, Z. Yu, R.M. Kil, Deep learning of support vector machines with class probability output networks, Neural Netw 64(2015) 19-28.

[14] A. Widodo, B.S. Yang, Support vector machine in machine condition monitoring and fault diagnosis, Mechanical Systems and Signal Processing 21(2007) 2560-2574.

[15] L.C. Jiao, S.Y. Yang, U.F. Li, Seventy years beyond neural networks: retrospect and prospect, Chinese Journal of Computers 39(8)(2016) 1697-1716.

[16] L.F. Chen, H.Y. M. Liao, M.T. Ko, A new LDA-based face recognition system which can solve the small sample size problem, Pattern Recognition 33(10)(2000) 1713-1726.

[17] A. Sharma, K.K. Paliwal, Linear discriminant analysis for the small sample size problem: an overview, International Journal of Machine Learning & Cybernetics 6(3)(2015) 443-454.

[18] H. Azami, J. Escudero, A. Humeau-Heurtier, Bidimensional distribution entropy to analyze the irregularity of small-sized textures, IEEE Signal Processing Letters 24(9)(2017) 1338-1342.

[19] S.D. Ridder, P. Manfredi, J.D. Geest, A generative modeling framework for statistical link analysis based on sparse data, IEEE Transactions on Components Packaging & Manufacturing Technology 8(1)(2018) 21-31.

[20] M. Ahadi, S. Roy, Sparse Linear Regression Approach for Efficient Multidimensional Uncertainty Quantification of High-Speed Circuits, IEEE Press, 2016.

[21] H.N. Liu, F.Z. Song, R. J. Dou, Y. X. Huang, C. L. Liu, Domain adaptive fault diagnosis based on the geodesic flow kernel under small data condition, Journal of Vibration and Shock 37(18)(2018) 36-42.

[22] Y. Tan, W.L. Sun, G.G. Wen, X. Huang, Fluctuation detection and fault diagnosis of rotating machinery, Journal of Vibration, Measurement＆Diagnosis 38(5)(2018) 1044-1050 +1086-1087.

[23] V.T. Tran, F. Althobiani, A. Ball, An approach to fault diagnosis of reciprocating compressor valves using Teager-Kaiser energy operator and deep belief networks, Expert Systems with Applications 41(9)(2014) 4113-4122.

[24] W. Chen, M. Saif, A novel fuzzy system with dynamic rule base, IEEE Transactions on Fuzzy Systems 13(5)(2005) 569-582.

[25] Y.R. Shi, H. Wu, Data aggregation for road functionality detection based on machine leaning and VANET, Journal of Computers 29(2)(2018) 161-173.

[26] C.S. Chen, Y.X. Xiang, Z.W. Cheng, Improved fault analysis on RSA based on non-invasive fault, Journal of Computers 29(2)(2018) 45-54.

[27] J.B. Xiong, Q.H. Zheng, Z.P. Peng, G. Sun, Y. Cai, Double sample data fusion method based on combination rules, IEEE Access 4(2016) 7487-7499.

[28] Z.W. Wang, Q.H. Zhang, J.B. Xiong, M. Xiao, G. Sun, J. He, Fault diagnosis of a rolling bearing using wavelet packet denoising and random forests, Sensors 17(17)(2017) 5581-5588. doi:10.1109/JSEN.2017.2726011.